ISIJ International, Vol. 54 (2014), No. 10, pp. 2294–2301

Effect of Sub-critical Tempering and Deep Cryogenic Treatment on Slurry Erosion of Cr–Mn–Cu White Cast Irons

Prabhat KUMAR,[1)] Kausik CHATTOPADHYAY[2)] and Indrajit CHAKRABARTY[2)]*

1) UG Student, Visveswarya National Institute of Technology, Nagpur, Maharashtra-440010 India. 2) Faculty, Dept. of Metallurgical Engineering, Indian Institute of Technology (Banaras Hindu University), Varanasi, Uttar Pradesh-221005 India.

(*Received on April 1, 2014; accepted on May 26, 2014*)

The effect of deep cryogenic treatment and air cooling subsequent to sub-critical tempering treatment on the structural evolution and the resulting wear performance of Cr–Mn–Cu white cast iron in sand-water slurry media were studied. The as-cast matrix of Cr–Mn–Cu white cast iron is predominantly austenitic which can be transformed to a martensitic matrix embedded with fine M_7C_3 carbides, by a sub-critical tempering treatment followed by air cooling. But the retained austenite is not totally converted. Quenching of alloy in liquid nitrogen bath after subcritical tempering enables more amount of transformation of austenite with simultaneous homogeneous precipitation of fine carbides. The phase transformation and corrosion-erosion behavior were characterized by optical and scanning electron microscopy, bulk and micro-hardness measurement and x-ray diffraction analysis, measurement of corrosion rate and slurry erosion test. The slurry erosive wear performance has been found to be much better in the cryotreated alloys compared to those with conventional sub-critically tempered alloys.

KEY WORDS: Cr–Mn–Cu white cast irons; cryogenic treatment; sub-critical tempering; corrosion; slurry-erosion.

1. Introduction

High chromium and nickel-chromium irons are the most potent erosion resistant ferrous alloys widely employed for slurry pumps, coal and cement grinding mills, ore comminution *etc.* Many of these applications involve a synergistic attack of erosion and corrosion.[1)] The composite- like microstructure in these alloy irons result in high wear resistance in which hard carbide phases are embedded in a tough matrix. The tough matrices which may be either the as-cast austenitic matrix or a predominantly martensitic matrix obtained by a suitable heat treatment support the hard carbides against wearing action. The tough matrices are also responsible for adequate toughness necessary to combat in-service impact actions. Further improvement in the aforesaid alloy iron properties can be achieved by a suitable alloying or by resorting to a proper heat treatment. The modifications through cheaper alloying additions like manganese and copper in chromium rich irons have been examined and proved to be beneficial.[2–6)] Manganese and copper both is being austenite stabilizer produce predominantly austenitic matrix in as-cast condition suppressing pearlite transformation, additionally copper improves corrosion resistance of the iron. In major corrosion-erosion applications the chromium is responsible to form a passive film of Cr_2O_3 that suppresses the mild corrosion and minimizes the synergistic effect of erosion and corrosion. Copper appears to act in the same way in the formation of passive film.[5)] The as-cast austenitic matrix can be further transformed to a hard martensitic matrix embedded with fine secondary alloy carbides by a suitable heat treatment. Such heat treatments are very often either a high temperature destabilization treatment or a sub-critical treatment.[7–10)] The sub-critical treatment has some specific advantages as it cuts down the cost of high temperature treatment and avoids distortions and fissuring of castings.[10)] But even after such conventional heat treatments the retained austenite cannot be fully converted to martensite. There has been a continuing interest to study the effect of cryogenic treatment on particularly die and tool steels and its effect on resulting wear behavior.[11–25)] In general, the effect of cryogenic treatment on different types of steels results in an extensive increase in wear resistance. This was attributed to complete transformation of austenite to martensite. Different mechanisms for microstructural evolution by cryo-treatment responsible for improved wear resistance are: 1) almost complete isothermal transformation of retained austenite to martensite below the martensite finish (Mf) temperature, 2) conditioning of martensite at low temperature involving sub-structural changes, 3) formation of higher volume percentage of refined uniformly dispersed secondary carbides due to lattice contraction and 4) better uniformity in dispersion than those with conventional heat treated steels.

In a recent study by Shaohong Li *et al.*[25)] have verified the mechanism of the refined carbide precipitation in tool steels on deep cryogenic treatment by internal friction method and transmission electron microscopy. The modification

* Corresponding author: E-mail: ichakraborty.met@itbhu.ac.in
DOI: http://dx.doi.org/10.2355/isijinternational.54.2294

© 2014 ISIJ

of secondary carbide precipitation is due to high internal stresses developed from austenite to martensite transformation. The interstitial carbon atoms are segregated at the nearby moving dislocations by the martensite lattice contraction. As a result, the lattice tetragonality becomes very low. A strong interaction between the time dependent strain field of dislocation and the segregated carbon atoms is produced. At the nearby dislocations the segregated carbon atoms form clusters which are forming nuclei for carbide precipitation during subsequent warming up to room temperature or tempering. These uniformly dispersed refined secondary carbides improve the wear and mechanical properties on deep cryogenic treatment.

Cryogenic treatment has also been employed to study the effect on microstructure and wear characteristics of high chromium irons by various researchers.[8,10,26–28] The findings show that cryogenic treatment after destabilization or sub-critical treatment, the retained austenite content is substantially reduced and transformed to martensite. The volume percentage of secondary carbide precipitation is more than that with air cooling. Consequently, the bulk hardness achieved is more and the resulting abrasion resistance is better with cryo-treatment.

As there is dearth of published information on the effect of deep cryogenic treatment on Cr–Mn–Cu alloy irons, the present study was aimed to investigate the microstructural evolution and the slurry-erosion behavior of Cr–Mn–Cu white cast irons subjected to deep cryogenic treatment subsequent to sub-critical tempering.

2. Experimental Procedure

The alloy iron with the chemical composition 2.8%C, 4.5%Mn, 1.8%Si, 8.9%Cr, 2.9%Cu, 0.038%S and 0.036%P was melted in a basic lined high frequency induction furnace. Cylindrical test bars (2 cm. diameter and 15 cm. long) and wear test specimens were cast in sodium silicate-CO_2 bonded sand molds at a pouring temperature of 1 500°C.

To select the optimum temperature range and time for sub-critical treatment, the as-cast alloy was initially subjected to isochronal and isothermal heat treatment. Isochronal tempering treatment in the sub-critical temperature range of 400, 500, 600 and 700°C were carried out for a fixed period of 1 hour and subsequently air cooled to room temperature. The effect of isothermal holding time at the optimum tempering temperature obtained from isochronal tempering were studied by isothermal tempering for various length of soaking time viz. 1,3 and 5 hours and subsequently either air cooled or quenched in liquid nitrogen bath and kept immersed for 30 minutes.

The microstructures were observed under optical microscope and scanning electron microscope. Vickers bulk hardness was measured with 30 kgf load. The reported hardness values for each sample are based on an average of ten readings at different locations; the mean of these readings are plotted with deviations in the error bar. The matrix microhardness at different heat treatment conditions were taken in Shimadzu make Vickers Microhardness Tester with 100 gm load. The retained austenite contents of a few samples were estimated by x-ray diffraction analysis with Cu Kα radiation. The effects of texture were eliminated by continuous rotation of the sample.

To determine the volume percent of carbides present in the alloy in different conditions, carbides were extracted electrolytically. These volume percent of carbides were computed to determine ultimately the retained austenite content in the matrix. The extraction were carried out in an electrolytic bath consisting of 5% concentrated HCl in ethyl alcohol with the sample as anode and a stainless steel plate as cathode. The extraction was continued for about 20 hours with a current density of 5 mA/cm^2 and the extracted carbides were collected in a glycerin layer at the bottom of the electrolyte. After extraction, the carbides were filtered off, rinsed thoroughly with ethyl alcohol, dried at 70°C and weighed accurately. The volume percent were calculated by a specific gravity bottle using glycerin to fill the bottle.

The rate of corrosion in tap water of heat treated samples were measured following standard ASTM immersion test (G-1-72). Mirror polished rectangular surface specimens prepared with 600 grit paper were cleaned with distilled water and finally with acetone, and then dried and weighed. The prepared samples were suspended in the tap water (pH= 7) for 168 hours at room temperature. The specimens were again cleaned, dried and weighed after the specified duration of immersion. The rate of corrosion was calculated using the relationship,

Corrosion rate [in mg/decimeter^2/day (mdd)] = K.w/(A.T.D)

Where, K= 2.4×10^6.D

W= weight loss in g nearest to 1 mg.

A= surface area in square cm nearest to 0.01 cm^2

T= duration in hours.

D= density of the material in g/cc.

The erosive wear characteristics were evaluated in a slurry pot tester as illustrated in **Fig. 1**. Although the effect of impact angle of the slurry particles cannot be evaluated in this test, the relative erosive wear characteristics of the test alloys in different heat treatment conditions can be well assessed under identical condition. The ground (with No. 1000 emery paper), cleaned (with water and acetone) and dried cylindrical specimens (10 mm. diameter and 50 mm. long) were fitted in the holding disc of the test rig. Two specimens of a particular heat treatment condition were placed at the two diametrically opposite positions to avoid any biasness. The slurry contained 60% by weight of silica sand particles in plain water. The silica sand used was with average size of 325 μm, roundness (Rettenhouse sphericity) 0.77 and microhardness 1 100–1 150 Kg/mm^2. The speci-

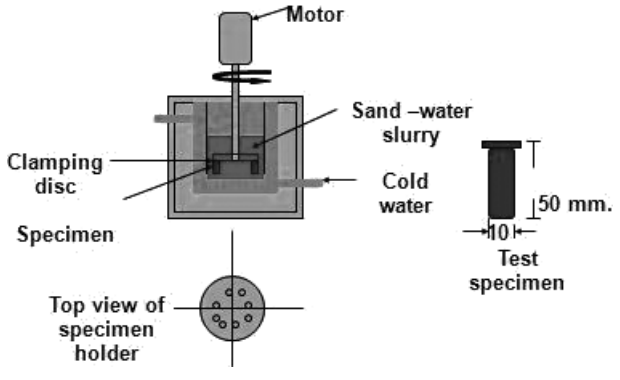

Fig. 1. Slurry erosion test set-up.

© 2014 ISIJ

mens were rotated in the slurry at 500 rpm corresponding to a linear speed of 4.5 m/s for a total duration of 24 hours. The mass losses of the cleaned, dried specimens were measured after every 6 hours of test run. The final worn out samples from the tip were cut off, cleaned ultrasonically in acetone and examined under scanning electron microscope for surface topography.

3. Results and Discussion

3.1. Phase Transformation Behavior

The as-cast Cr–Mn–Cu white cast irons comprise of predominantly austenitic matrix with discontinuous primary eutectic M_7C_3 carbides (**Fig. 2**(a)). The x-ray diffraction pattern of the corresponding alloy is shown in **Fig. 3**. The austenite content has been measured to be around 83%. The volume percentage of the carbides determined from electrolytic extraction of carbides is 14.34%.

The bulk hardness versus tempering temperature curve corresponding to the isochronal tempering of as-cast alloy and subsequent air cooling is shown in **Fig. 4**. The figure indicates that the bulk hardness attains a maximum at the temperature around 600°C and decreases with further increase in tempering temperature. The corresponding optical micrographs are shown in Fig. 2, which reveal that as-cast austenitic matrix gradually transformed into a dark martensitic phase embedded with fine alloy carbides. The attainment of peak hardness at around 600°C can be attributed to two reasons; 1) due to precipitation of fine secondary alloy carbides the austenitic matrix gets depleted of alloying elements and as a consequence the martensitic start temperature (Ms) is raised. So, during air cooling to room temperature the alloy depleted austenite is converted to martensite embedded with fine alloy carbides; 2) the precipitation hardening due to fine alloy carbides. With further rise in isochronal tempering temperature the bulk hardness decreases due to two reasons- the matrix is converted to ferrite-carbide aggregate and the coarsening of the secondary alloy carbides.

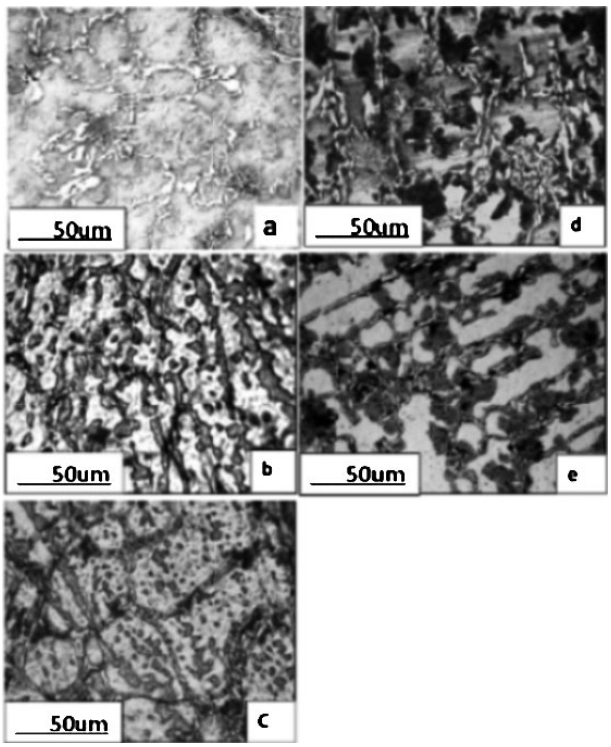

Fig. 2. Optical micrographs of a) as-cast alloy; b), c), d) and e) are isochronally tempered alloy at 400°, 500°, 600° and 700°C respectively for 1 hour.

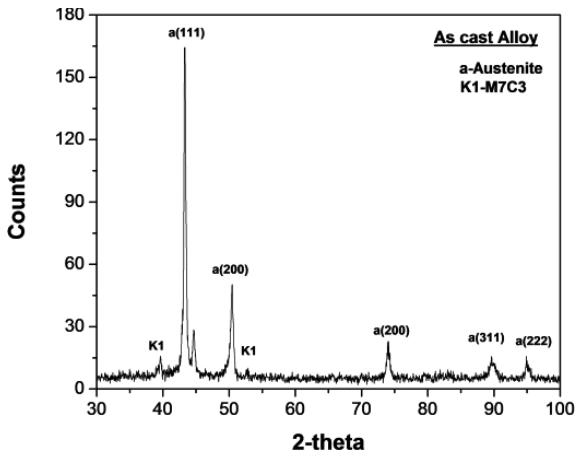

Fig. 3. XRD profile of as-cast alloy.

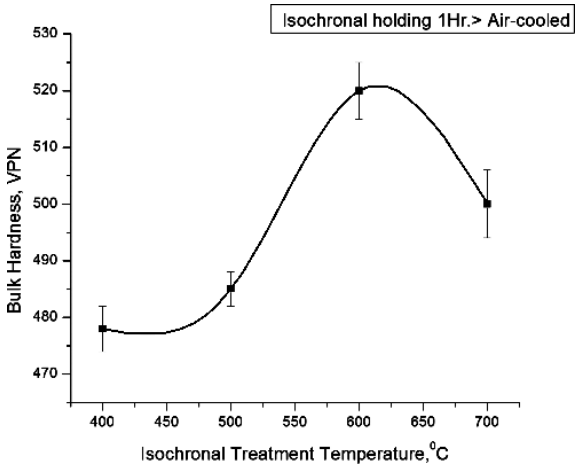

Fig. 4. Bulk hardness versus isochronal tempering temperature plot.

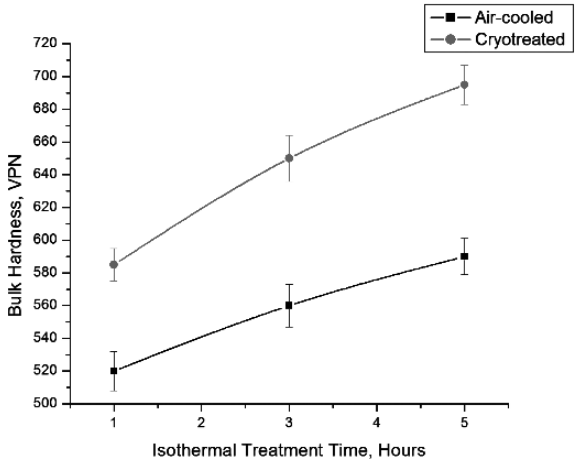

Fig. 5. Bulk hardness versus isothermal treatment (600°C) time plot.

© 2014 ISIJ

The bulk hardness versus isothermal tempering time curves for subsequent air cooling and cryogenic treatment have been shown in **Fig. 5**. The corresponding optical micrographs and scanning electron micrographs are shown in **Figs. 6** and **7** respectively. From the microstructures and the retained austenite content measurement from XRD analysis (**Fig. 8**), it is evident that, although the cryotreatment could not eliminate the retained austenite content with 5 hours of tempering, it is more effective in reducing the retained austenite content than that in isothermal tempering and air cooling. The SEM micrographs of the cryotreated samples show that the ultrafine carbide distribution becomes more homogeneous. During the cryotreatment the structure is believed to be contracted and some new defects such as dislocations, as-quenched vacancies and twins are introduced. These defects attract carbon atoms from the saturated and contracted martensites. During subsequent warming up to the room temperature these are acting as preferential sites for further finer carbide nucleation which increases the carbide volume percentage as well as homogeneous distribution.[24,25] Moreover, the increase in the amount of finer secondary carbide precipitates in cryotreatment contributes to the increase in the dispersion strengthening effect. The microhardness values at different tempering time also substantiate these effects as depicted in **Table 1**.

In a separate study carried out by one of the authors,[28] almost the same alloy iron was destabilized and deep cryotreated from a higher temperature of 750°C. While the transformation of retained austenite after sub-critical tempering treatment is compared with that in the alloys after high temperature destabilization treatment at 750°C, it is observed that the retained austenite contents are much lower after high temperature treatments. After destabilization at 750°C for 9 hours followed by air cooling the retained austenite content is only 12% and in cryotreated alloy it is totally zero. So, it appears that, high temperature destabilization is more efficient in reduction of retained austenite compared to sub-critical tempering treatment. However, subcritical

Table 1. Details of matrix microhardness, carbide volume% and retained austenite% of alloys.

Alloy condition	Matrix microhardness, (HV0.1)	Carbide volume%	Retained austenite%
a) As-cast	525 ± 18	14.34	82.86
b) Isothermally tempered at 600°C for 5 hours → air cooled	680 ± 15	24.53	26.90
c) Isothermally tempered at 600°C for 5 hours → cryotreated	772 ± 20	29.76	19.96

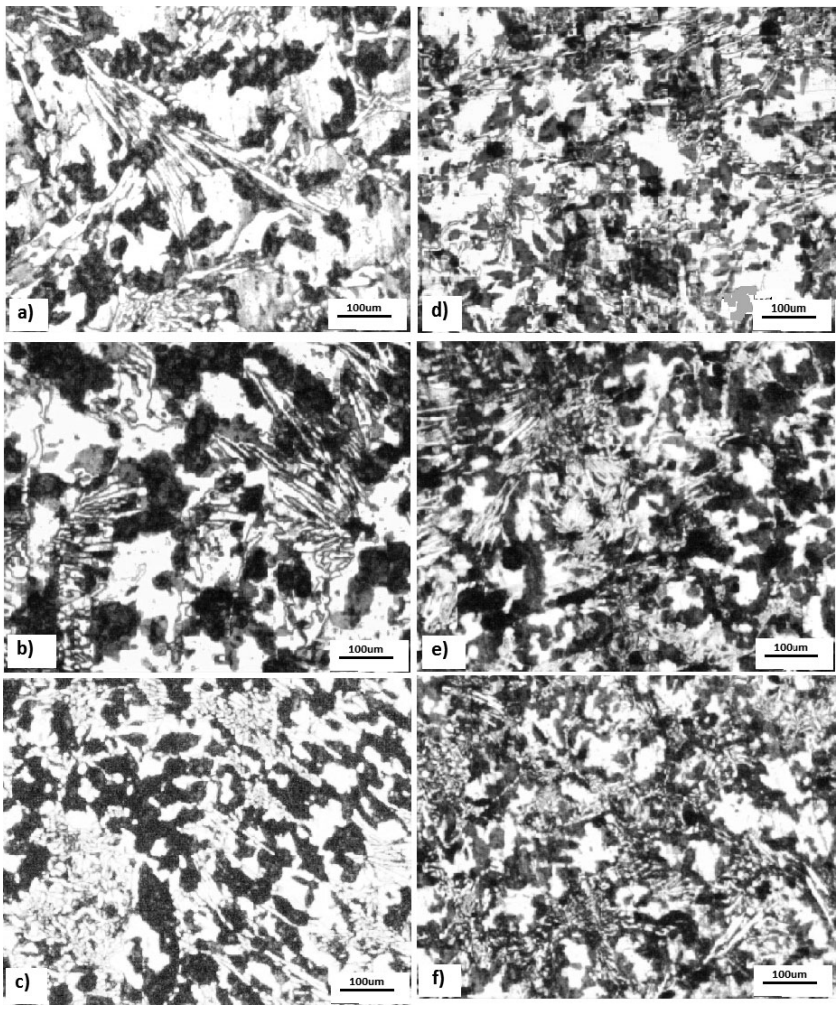

Fig. 6. Optical micrographs of isothermally tempered alloy at 600°C for a) 1 hour; b) 3 hours; c) 5 hours respectively and air cooled and d), e) and f) are the tempered and cryotreated.

© 2014 ISIJ

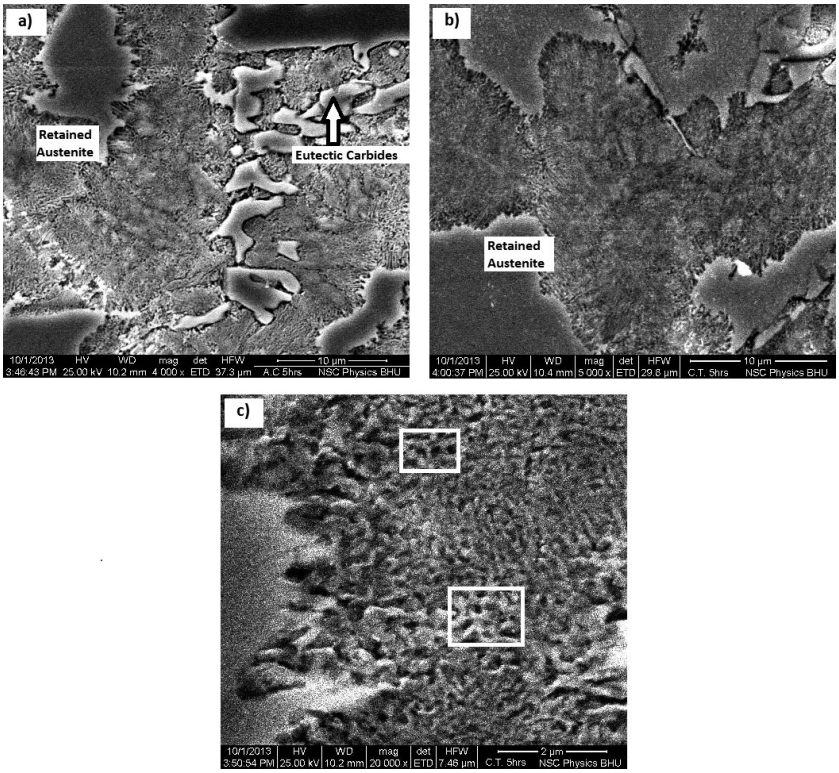

Fig. 7. SEM of subcritically tempered (600°C for 5 hours) and subsequently a) air cooled; b) cryotreated and c) cryotreated alloy at higher magnification showing ultrafine carbide precipitates in the matrix.

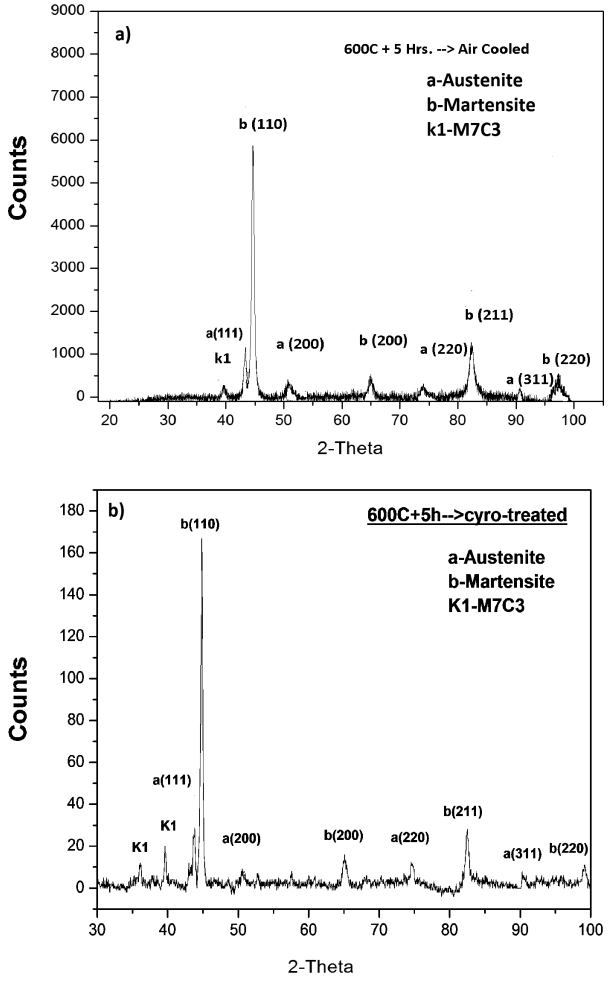

Fig. 8. XRD profile of tempered and a) air cooled and b) cryotreated alloy.

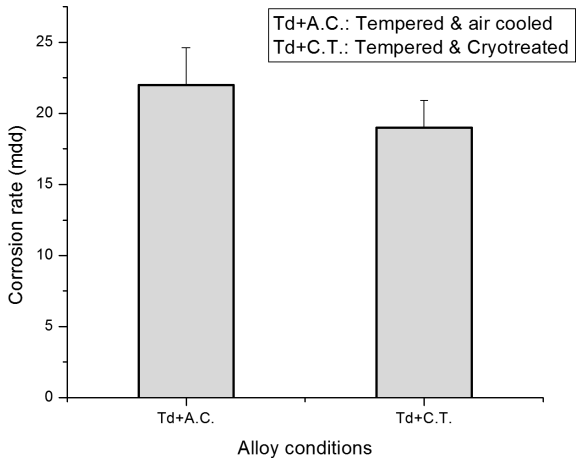

Fig. 9. Effect of alloy conditions on the corrosion rate in tap water.

deep cryogenic tempering treatment due to its specific advantages with respect to reduced treatment cost and absence of distortion and fissuring of castings are definitely favorable points towards the selection of treatment process.

3.2. Corrosion Rate

The static corrosion rates of sub-critically tempered and subsequently air cooled and cryotreated alloys in tap water (pH =7) is shown in **Fig. 9**. Cryotreated alloy shows a lower rate of corrosion than that of tempered and air cooled alloy. Similar improvement in corrosion resistance has been observed by Amini *et al.* in cryotreated tool steel[24] and Vidyarthi *et al.* in destabilized and cryotreated Cr–Mn–Cu white cast iron.[28] The improvement in corrosion resistance has been attributed to the more uniform carbide distribution

© 2014 ISIJ

in association with higher fine carbide formation in cryotreated alloys. It is believed that, the deep cryogenic treatment reduces the internal stress and stabilizes the dislocation structure resulting in the decreasing free energy of atoms and better corrosion resistance.[28–30)]

3.3. Slurry Erosion Behavior

The cumulative wear loss versus time curves have been shown in **Fig. 10**. It is apparent from this plot that, the wear resistance of the cryotreated samples is significantly improved compared to those in air cooled samples after sub-critical treatment. The microhardness of the matrix appears to play an important role in decreasing the rate of wear. The corresponding microstructure obviously will have a great influence on the wear loss. A uniform predominantly martensitic matrix embedded with fine and hard alloy carbides exhibit good wear resistance. The better wear resistance of cryotreated samples can be attributed to four factors.[12)]

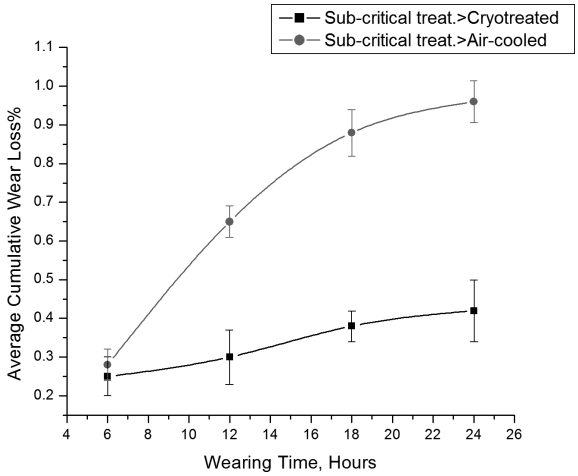

Fig. 10. Average cumulative wear loss with time.

Firstly, due to reduction of retained austenite and its conversion to higher percentage of martensite in the matrix this provides stronger support to the hard and fine secondary alloy carbides during erosion. Secondly, more homogeneous precipitation with high volume fraction of finer alloy carbides. Thirdly, cryotreatment produces refined martensitic matrix causing a fine grain strengthening effect and this improves the wear resistance further and lastly the improvement in corrosion resistance.

The worn out surface topography have been analyzed using Scanning Electron Microscope (SEM). The SEM micrographs show (**Fig. 11**) formation of indentation craters caused by plowing mechanism as suggested by Hutchings.[31)] The erodents which are rounded to sub-angular in shape, impact on the material surface pushing the material in the direction of movement of the erodent forming a lip ahead of the erodent. The erosion occurs due to fracture and detachment of this lip. The material is displaced also at the sides of the impact craters. In case of sub-critically tempered and air cooled alloys, the plowings are more prominent and the primary eutectic carbide cluster areas are less worn out as those are seen in relief (Fig. 11). Effect of corrosion attack at the matrix/eutectic carbide interface is prominent (**Fig. 12**). Since the corrosion potential of the carbides is believed to be nobler than the matrix, the matrix acts as a sacrificial anode. The carbon and chromium depleted zones around the eutectic carbides are responsible for main corrosion attack. Due to the effect of corrosion the eutectic carbides can lose their supports from the matrix and the carbides can be more easily fractured or removed by erosion. When the sand particles in the slurry impact carbides, cracks formed around and at the base of a wear groove which further lead to spall formation and hence material removal. Similar type of material removal mechanism may be operative for secondary carbides. The presence of more amount of retained austenite in the matrix might have aggravated this fine crack formation since any strain induced martensite formation at the

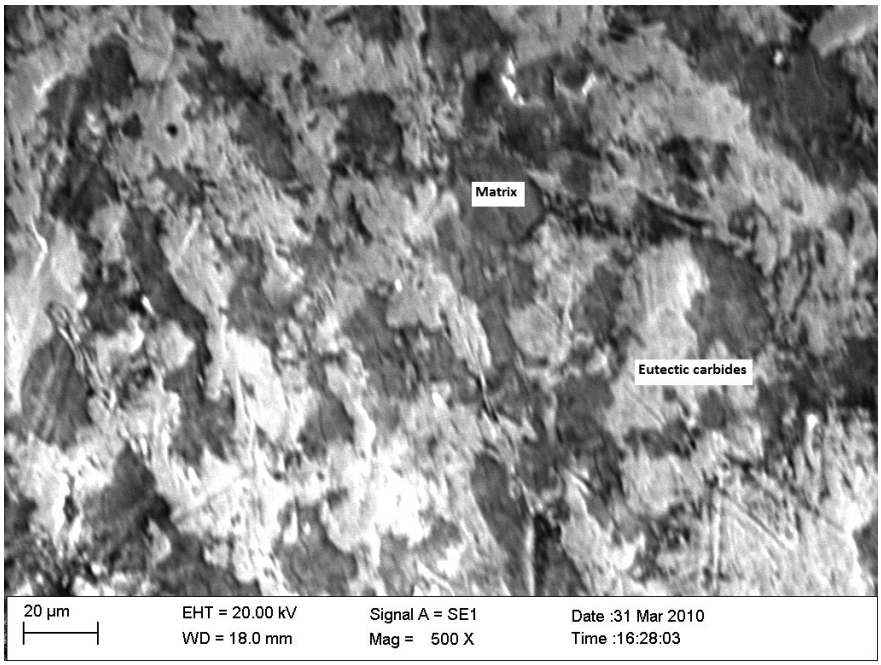

Fig. 11. SEM of worn surface of subcrtically tempered and air cooled alloy.

© 2014 ISIJ

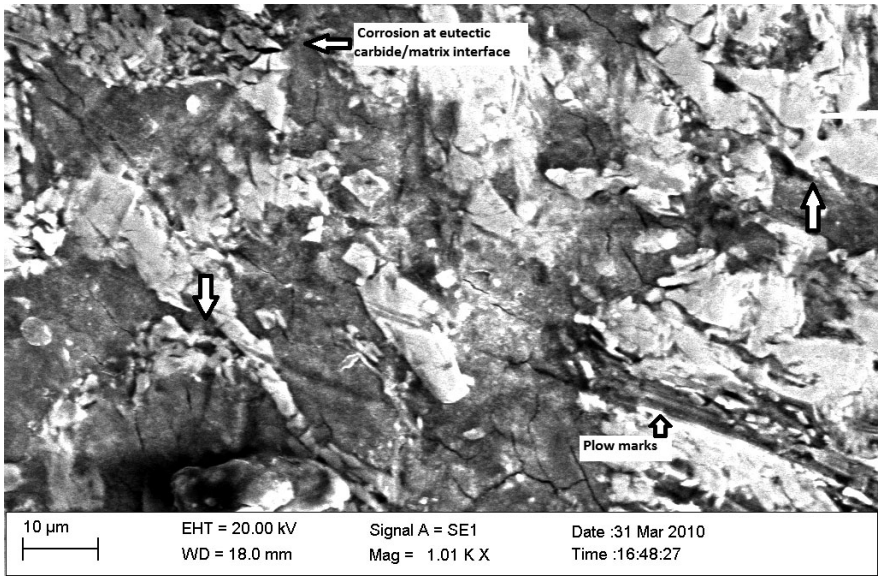

Fig. 12. SEM of the same sample showing corrosion attack at the matrix/eutectic carbide interface and plow marks by the erodent.

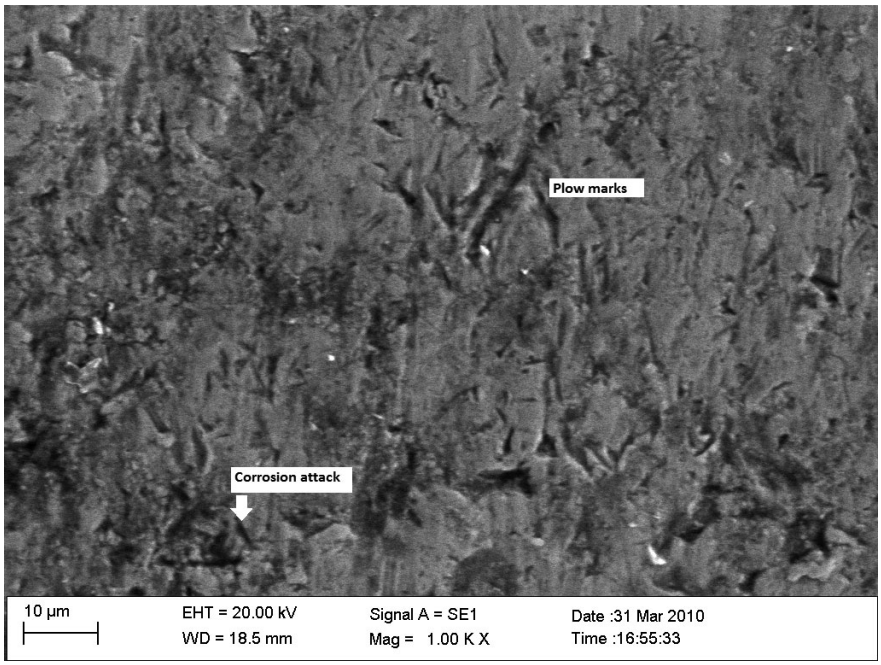

Fig. 13. SEM of the worn surface of subcritically tempered and cryotreated sample.

surface by the erodent impact causes volume expansion and a tensile stress is developed at subsurface. Matrix microcracks are seen in Fig. 12 which are subsequently detached to form craters. In contrast, worn surfaces of cryotreted samples are smoother (**Fig. 13**) which can be attributed to their better erosion resistance resulted from higher matrix microhardness and lesser retained austenite content. Along with higher erosion resistance, improved corrosion resistance property results in shallow penetration and hence lesser erosion-corrosion synergism.

4. Conclusions

(1) Cryogenic treatment is more efficient than the conventional isothermal subcritical tempering and subsequent air cooling in decreasing the retained austenite content and their consequent transformation to fine martensite phase embedded with ultrafine secondary carbide precipitates.

(2) Both the amount and fineness of secondary alloy carbide precipitations are increased by cryotreatment.

(3) The static corrosion rate of subcritically tempered and cryotreated alloy in tap water is better than that of tempered and air cooled alloy.

(4) The hardness and the resistance to slurry erosion both are found to be improved in cryotreated alloys compared to their counterpart due to the development of favorable microstructure.

© 2014 ISIJ

REFERENCES

1) T. A. Adler and O. N. Dogan: *Wear*, **225** (1999), 174.
2) A. Basak, J. Penning and J. Dilewijns: *Int. Cast Met. J.*, **16** (1981), 12.
3) I. Chakrabarty and A. Basak: *AFS Trans.*, **98** (1990), 707.
4) G. J. Cox: *Br. Foundrym.*, **76** (1983), 129.
5) I. Chakrabarty: *Int. J. Met. Cast.*, Winter (2011), 49.
6) I. Chakrabarty, A. Basak and U. K. Chatterjee: *Wear*, **143** (1991), 203.
7) C. P. Tabrett and I. R. Sare: *Wear*, **203–204** (1997), 206.
8) C. P. Tabrett and I. R. Sare: *Scr. Mater.*, **38** (1998), 1747.
9) C. P. Tabrett, I. R. Sare and M. R. Ghomashchi: *Int. Mater. Rev.*, **41** (1996), 59.
10) H. Liu, J. Wang, H. Yang and B. Shen: *Mater. Sci. Eng. A*, **478** (2008), 324.
11) D. N. Collins: *Heat Treat. Met.*, **2** (1996), 40.
12) D. Das, A. K. Dutta, V. Toppo and K. K. Ray: *Mater. Manuf. Process.*, **22** (2007), 474.
13) D. Das, R. Sarkar, A. K. Dutta and K. K. Ray: *Mater. Sci. Eng. A*, **528** (2010), 589.
14) A. Joseph Vimal, A. Bensely, D. Mohan Lal and K. Srinivasan: *Mater. Manuf. Process.*, **23** (2008), 369.
15) N. S. Kalsi, R. Sehgal and V. S. Sharma: *Mater. Manuf. Process.*, **25** (2010), 1077.
16) M. Arockia and D. Mohan Lal: *Mater. Manuf. Process.*, **25** (2010), 842.
17) M. Koneshlou, K. M. Asl and F. Khomamizadeh: *Cryogenics*, **51** (2011), 55.
18) K. Amini, S. Nategh and A. Shafyei: *Mater. Design*, **31** (2010), 4666.
19) D. Senthilkumar and I. Rajendran: *Mater. Manuf. Process.*, **27** (2012), 567.
20) M. El Mehtedi, P. Ricci, L. Drudi, S. El Mohtadi, M. Cabibbo and S. Spigarelli: *Mater. Design*, **33** (2012), 136.
21) R. Sri Siva, A. Arockia Jaswin and D. Mohan Lal: *Tribol. Trans.*, **55** (2012), 387.
22) M. Arockia Jaswin and D. Mohan Lal: *Mater. Design*, **32** (2011), 2429.
23) P. Baldissera: *Mater. Design*, **31** (2010), 4725.
24) K. Amini, A. Akhbarizadeh and S. Javadpour: *Mater. Design*, **45** (2013), 316.
25) S. Li, N. Min, J. Li, X. Wu, C. Li and L. Tang: *Mater. Sci. Eng. A*, **575** (2013), 51.
26) H.-S. Yang, J. Wang, B.-L. Shan, H. Liu, S.-J. Gao and S.-J. Huang: *Wear*, **261** (2006), 1150.
27) H. Liu, J. Wang, B.-L. Shan, H.-S. Yang, S.-J. Gao and S.-J. Huang: *Mater. Design*, **28** (2007), 1059.
28) M. K. Vidyarthi, A. K. Ghose and I. Chakrabarty: *Cryogenics*, **58** (2013), 85.
29) R. F. Barron and R. H. Thompson: Proc. of Int. Cryogenic Materials Conf., Paper BP-17, Plenum Press, New York, (1989), 187.
30) F.-Z. Xuan, X. Huang and S.-T. Tu: *Mater. Design*, **29** (2008), 1533.
31) I. M. Hutchings: Tribology – Friction and Wear of Engineering Materials, Edward Arnold, London, (1992), 175.

© 2014 ISIJ